



# Synthesis, Spectroscopic, Optical, and Thermal Characterizations of Zinc (Tris)-Thiourea Sulfate: A Metal-Organic Crystal

Helen Merina Albert<sup>1</sup> · T. Jemima<sup>1</sup> · C. Alosious Gonsago<sup>2</sup>

Received: 29 May 2023 / Accepted: 30 June 2023 / Published online: 15 July 2023

© The Author(s), under exclusive licence to Springer Science+Business Media, LLC, part of Springer Nature 2023

## Abstract

In the current research, Zinc (tris)-thiourea sulfate (ZTTS), a metal-organic crystal, has been synthesized using the slow solvent evaporation technique. Powder-X-ray diffraction (PXRD) analysis, Fourier transform infrared (FT-IR) spectroscopy, UV-Vis spectroscopy, photoluminescence (PL) spectroscopy, and thermal, and second harmonic generation measurements have all been applied to describe the as-synthesized ZTTS crystals. The synthesized samples crystallized in an orthorhombic structure, based on XRD analysis. The functional groups of ZTTS samples were validated by FT-IR analysis. The extensive transparency of ZTTS over the UV-visible spectral region has been confirmed by UV-Vis analysis and the band gap has been estimated as 4.43 eV. The photoluminescence spectra exhibit a prominent emission peak around the wavelength of 484 nm and significant emission peaks at 444 and 513 nm with an excitation wavelength of 250 nm. The SHG test illustrates the creation of second harmonic signals from the ZTTS samples. The thermal response of the as-synthesized ZTTS was shown by the TG/DTA measurements. The results suggest that as-synthesized ZTTS crystals could be used as a possible nonlinear optical substance.

**Keywords** Synthesis · XRD · FT-IR · UV · Photoluminescence · TG/DTA

## Introduction

Nonlinear optics deals with the study of the interaction of strong electromagnetic fields with substances to generate modified electromagnetic fields that differ from the original fields in terms of amplitude, wavelength, and phase. Nonlinear optics is mainly interesting because of its prospective uses in sensor applications, optical data storage, optical processing, and optical computing [1–3]. Numerous studies have been conducted on second harmonic generation (SHG), a crucial nonlinear property of noncentrosymmetric crystals [4–8]. Laser development, optical capacity

development, and electro-optic adjustment are all significantly influenced by non-linear optical substances. Hence, it is essential to keep developing new classes of nonlinear optical substances that are appropriate for frequency conversion in the UV to near-IR spectral regions. Finding and synthesizing novel optical crystals with good crystalline nature has emerged as an intriguing branch in crystal growth to satisfy the growing need for new materials with strong optical properties. Organic crystals are used as model systems to explore the effects of ion impact. When compared with inorganic compounds, organic compounds can frequently satisfy these stipulations; nevertheless, they also have several disadvantages, including poor chemical and mechanical stability, feeble laser damage thresholds, and inadequate phase-matching capabilities.

The development of metal-organic crystals has recently gained importance to get around these disadvantages. Due to their enhanced optical performance, stronger chemical strength, and higher mechanical stiffness compared to organic substances, metal-organic crystals have drawn a lot of interest [9–11]. Thiourea compounds play a significant role among metal-organic compounds due to their excellent non-linear efficiency, wider transparency, and excellent

✉ C. Alosious Gonsago  
c.alosious@gmail.com

Helen Merina Albert  
drhelenphy@gmail.com

T. Jemima  
tjrmima@gmail.com

<sup>1</sup> Department of Physics, Sathyabama Institute of Science and Technology (Deemed to Be University), Chennai, India

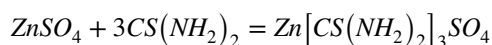
<sup>2</sup> Department of Electronics Science, Mohamed Sathak College of Arts and Science, Chennai, India

thermal and mechanical strength. With its capacity to produce a vast hydrogen bond network and strong dipole moment, the ligand thiourea is an exceptional chemical compound [12]. The metallic substances, however, easily coordinate with thiourea and acquire the noncentrosymmetric structure which is the essential condition for obtaining excellent optical transparency and sufficient nonlinear response. Numerous thiourea metallic complexities have been developed and thoroughly investigated, including cadmium thiourea acetate, potassium thiourea chloride, thiourea urea zinc sulfate, zinc thiourea chloride, calcium bis-thiourea chloride, bis-thiourea cadmium chloride, bis-thiourea cadmium iodide, Bis-(thiourea) strontium chloride, bis-thiourea zinc acetate, bis-(thiourea) zinc carbonate, 2-aminopyridine bis-thiourea zinc sulfate, tris-thiourea magnesium zinc sulfate, Zinc-(Tris) thiourea chloride, and Tetrakis-(thiourea) cobalt chloride [13–26].

Zinc thiourea sulfate is one of the promising thiourea-metal compounds that were initially reported by Andreotti et al. [27]. The purpose of the current investigation is to build high-quality NLO crystals of thiourea and zinc coordination. Growing crystals from aqueous solutions is a prominent method of crystal development that has produced a number of technologically relevant crystals [28]. Thus, zinc (tris)-thiourea sulfate (ZTTS) single crystals have been synthesized at room temperature using the slow evaporation approach. This paper describes the synthesis of ZTTS and its spectral, optical, and thermal characteristics.

## Materials and Methods

Zinc tris-thiourea sulfate (ZTTS) single crystals were synthesized from an aqueous solution using a slow solvent evaporation process. The starting material was created by dissolving appropriate volumes of zinc sulfate (AR grade) and thiourea in deionized water at a 1:3 molar ratio. The following chemical process is anticipated to occur in deionized water:



To get a uniform mixture, the produced solution was thoroughly agitated for over six hours using a magnetic stirrer. Super-saturation was achieved by gradually heating the combination to a temperature below 60 °C. After that, filter sheets were used to eliminate any undesired contaminants. The filtered ZTTS solution was stored in a vessel for crystallization, closed with a perforated sheet, and placed in a space free of dust. By slowly evaporating the solvent, the crystals were developed in the crystallizing jar. A good single crystal of the ideal size was produced in 30 days at

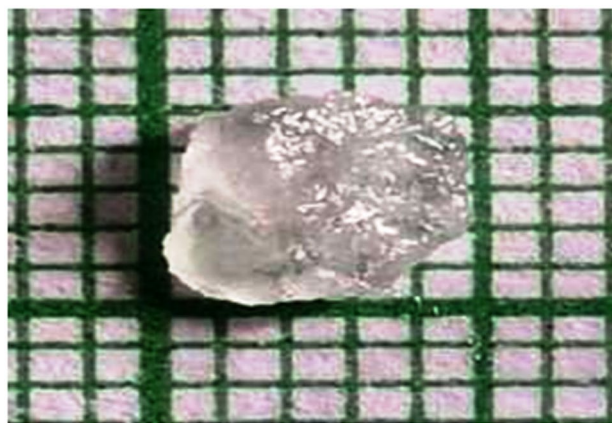


**Fig. 1** Image of an as-synthesized single crystal of ZTTS

room temperature (32 °C). Figure 1 depicts the image of an as-synthesized ZTTS single crystal.

## Characterization Techniques

Characterization essentially comprises assessing the chemical composition, optical properties, and thermal characteristics of the crystals. Powder-XRD, FT-IR, UV-Vis, PL investigations, SHG testing, and thermal characterizations were employed to examine the physicochemical characteristics of the ZTTS samples. Powder X-ray diffraction studies were performed using a Reich-Seifert 3003-TT diffractometer with a 1°/min scan speed. FT-IR spectroscopy was conducted using Perkin Elmer–Spectrum-II spectrometer to identify functional groups found in the ZTTS sample. Finely powdered samples were used for this analysis and the spectra were obtained in the region of 400–4000 cm<sup>-1</sup>. The UV-Vis absorbance spectra of ZTTS samples were obtained using a Jasco V-670 spectrophotometer between the wavelength ranges of 200 and 800 nm at a data interval of 1 nm and 400 nm/min scan rate. The PL studies were conducted using a Perkin Elmer-LS45 fluorescence spectrophotometer in the wavelength range of 200–900 nm to quantify the fluorescence parameters, including its intensity and wavelength distribution after being excited by a specific light spectrum. The powder method of Kurtz and Perry was followed to identify the SHG of the samples. A Q-switched High Energy Nd: YAG Laser (QUANTA RAY Model LAB –170–10) Model HG-4B-high efficiency, angle tuned and temperature stabilized Second harmonic of energy 450 mJ was employed for SHG measurements. The thermal studies were carried out between 50 and 800 °C in nitrogen gas at a 20 °C/min heat flow using a Perkin Elmer STA6000 thermal analyzer.

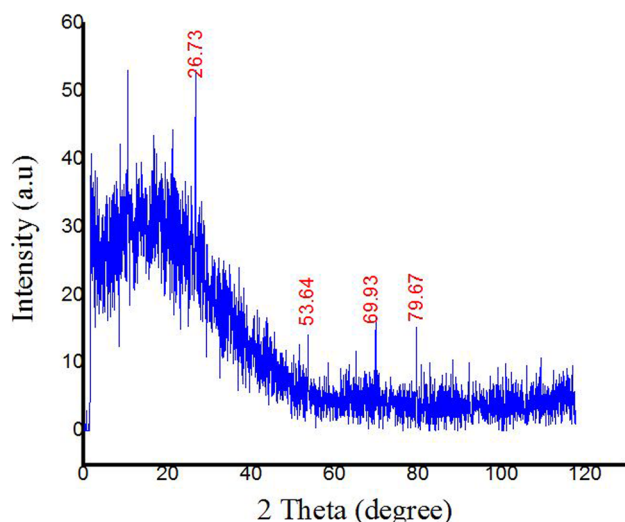


Fig. 2 Powder-XRD pattern of ZTTS

## Results and Discussion

### Powder XRD Analysis

The X-ray diffraction analysis was performed to establish the structural form as well as to find the unit cell dimensions of the given compound [29]. The ZTTS sample was scanned by an X-ray of wavelength 1.5405 Å at a rate of 1 scan per minute across 1–120° orientations. The diffractogram of the powdered ZTTS sample is given in Fig. 2. Using the PROSZKI software program, the unit cell dimensions were estimated from the prominent peaks. According to P-XRD analysis, the ZTTS crystallized in an orthorhombic crystal formation. Four prominent peaks at orientations of 26.73°, 53.64°, 69.93°, and 79.67° have been identified. The peak located at 26.78° has the highest intensity per sec. The P-XRD test shows that the diffraction peaks and the orthorhombic shape of the ZTTS crystal are in good accord.

The lattice parameters were calculated using the following equations:

$$\text{Interplanar spacing, } d = \frac{n\lambda}{2 \sin \theta} \quad (1)$$

$$\text{Lattice constant, } a = d\sqrt{h^2 + k^2 + l^2} \quad (2)$$

$$\text{Average grain size, } D = \frac{0.89\lambda}{\beta \cos \theta} \text{ nm} \quad (3)$$

where,  $d$  is the d-spacing and  $h k l$  are the Miller indices,  $D$  is the average size (nm),  $\lambda$  is the Cu-K $\alpha$  radiation wavelength (Å),  $\beta$  is the full width at half-maximum (radian) and

$\theta$  gives the degree of scattering (degree). The estimated lattice parameters are  $a = 7.752 \text{ \AA}$ ,  $b = 11.171 \text{ \AA}$ ,  $c = 15.482 \text{ \AA}$ , and cell volume  $V = 1340.704 \text{ \AA}^3$ , which are consistent with previous studies [30].

The molecular structure of ZTTS is displayed in Fig. 3. The ZTTS sample crystallized in a noncentrosymmetric space group. The structure includes three thiourea units and an  $(\text{SO}_4)^{2-}$  unit. In each thiourea unit, one carbon atom is linked with a sulphur atom and two nitrogen atoms. Each nitrogen atom in turn bonded with two hydrogen atoms. The  $\text{Zn}^{2+}$  ion in the assembly is tetrahedrally paired with three sulfur atoms of the three units and an oxygen atom in the sulfate anion. An interesting hydrogen bonding network can also be found in the ZTTS structure. The hydrogen atoms in the network formed an intramolecular H-bonding with a sulfate ion and thiourea units.

### FT-IR Analysis

FT-IR spectroscopy is a powerful tool used to identify the various kinds of chemical bonds that can be found in a substance. FT-IR spectroscopy is applied to discriminate between organic and inorganic compounds. FT-IR absorption bands are used to identify certain compounds and their constituents [31, 32]. The FT-IR spectra of ZTTS samples are displayed in Fig. 4. The spectra show prominent peaks at 3368, 3271, 3166, 2112, 2036, 1820, 1589, 1468, 1385, 1089, 731, 622, and 486  $\text{cm}^{-1}$  respectively. The asymmetric and symmetric stretching frequencies of the  $\text{NH}_2$  group are resolved at 3368 and 3271  $\text{cm}^{-1}$ . The peak at 3166  $\text{cm}^{-1}$  is

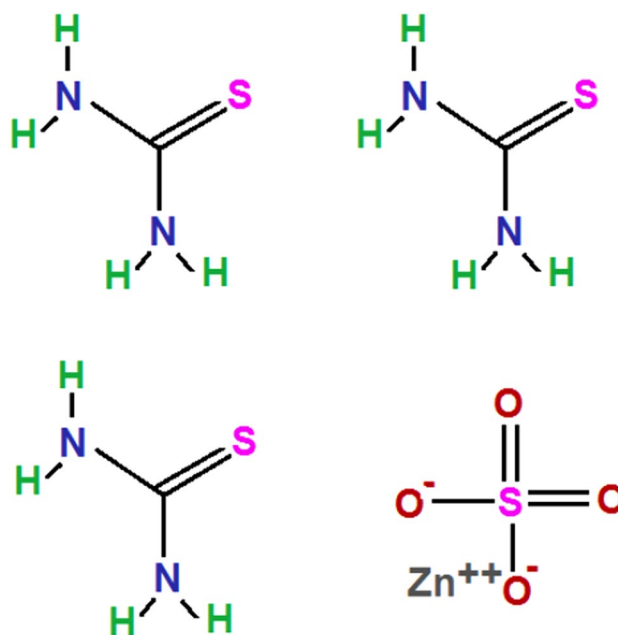
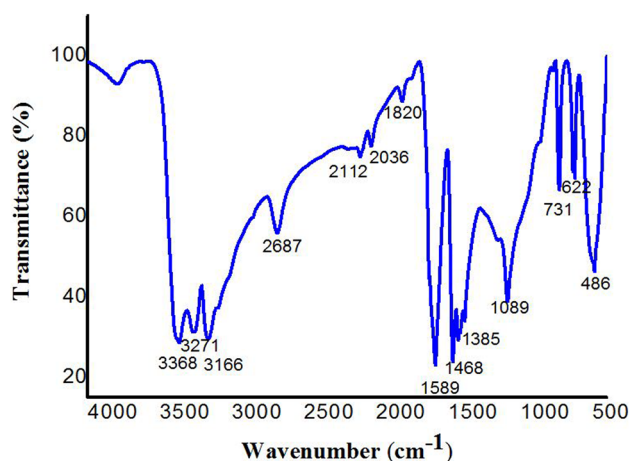


Fig. 3 Molecular structure of ZTTS



**Fig. 4** FT-IR curve of ZTTS

responsible for the O-H stretching vibration. The asymmetric and symmetric stretching of C-N has been responsible for the peaks at 2112 and 2036  $\text{cm}^{-1}$ , respectively. The N-H bending vibration has been found at 1820  $\text{cm}^{-1}$ . An intensive peak at 1589  $\text{cm}^{-1}$  is due to the N-H bending of the primary amine. The asymmetric and symmetric C=S stretching of thiourea are observed in the peaks at 1468 and 731  $\text{cm}^{-1}$ . The interaction of zinc with thiourea via the sulfate ion has been shown by the C=S stretching at 1089  $\text{cm}^{-1}$ . The S-C-N symmetric bending vibrations of thiourea are displayed at 486  $\text{cm}^{-1}$ .

### UV-Vis Analysis

The UV-Vis Spectroscopy technique is used to recognize, confirm, and measure a material's chemical, molecular, and structural characteristics [33]. The UV-Vis spectrum of

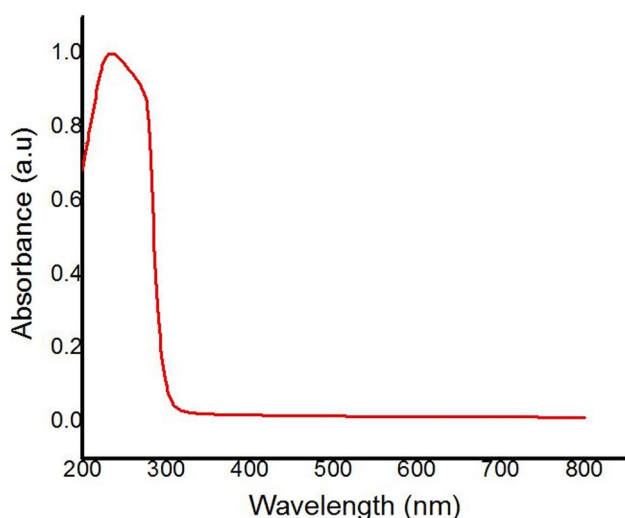


**Fig. 5** UV-Vis spectrum of ZTTS

the ZTTS is depicted in Fig. 5. The spectra show a small absorption in the near UV, visible, and near-infrared spectral areas. In other words, the optical transmittance of ZTTS is very high in the near-UV and visible ranges with the lower cut-off wavelength found at 280 nm. This is a constructive attribute of NLO systems since greater optical transparency in these regions improves the frequency conversion ability. The bandgap ( $E_g$ ) of ZTTS was calculated from the lower cutoff wavelength (280 nm) and can be generally found by the formula:

$$E_g = \frac{1240}{\lambda} \text{eV.}$$

where,  $E_g$  is the bandgap (eV), and  $\lambda$  is the wavelength corresponding to the limiting wavelength (nm). The bandgap at the 280 nm absorption limit is 4.43 eV. A higher bandgap of ZTTS is crucial for functioning at higher temperatures. Due to their ability to function at higher temperatures, these samples are most important in device applications.

### Photoluminescence (PL) Spectroscopy

Photoluminescence spectroscopy offers information regarding the structure, energy gap, localized flaws, and impurity concentrations in semiconducting substances. Photoluminescence (PL) spectroscopy is a non-invasive and non-contact technique for examining the optoelectronic properties of substances [34–36]. Photo-excitation occurs when light falls on a sample in which it is absorbed and gives excess energy to the substance. The readily available electrons are stimulated into their excited states by a high-energy lighting source. Light radiation is produced when these electrons with excess energy reach their equilibrium states. The energies of the released photons are related to the difference

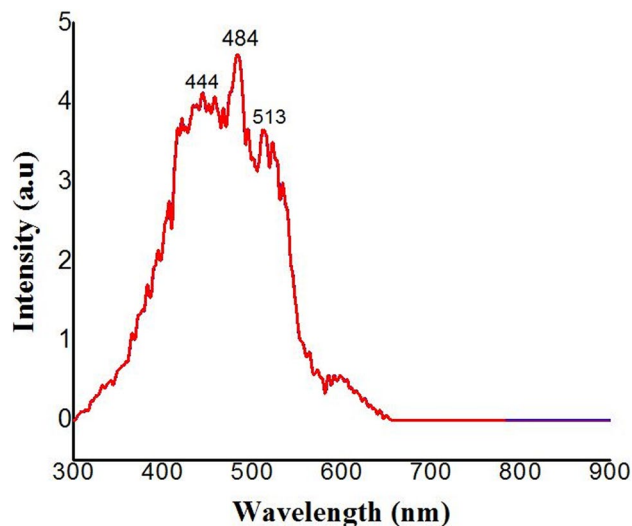


**Fig. 6** PL spectra of ZTTS

in energy levels between the two electronic states involved in the phase of transition. An optical spectrometer is used to find the intensity of the emitted photons related to their wavelength. The PL measurements were used to examine the emission characteristics of ZTTS. The PL spectrum was obtained for ZTTS in the 300–900 nm spectral range, with an excitation wavelength of 250 nm and photon energy of 4.96 eV. The obtained PL spectrum of ZTTS was depicted in Fig. 6. From Fig. 6, it has been observed that the prominent photoemission peak of ZTTS is centred on 484 nm with the highest intensity. Significant peaks are observed around 444 nm in the blue emission and 513 nm in the green emission regions. The green emission can be attributed to the  $\pi \rightarrow \pi^*$  transition due to the interaction of  $\text{Zn}^{2+}$  and thiourea molecules. In this study, several minute peaks between 400 and 550 nm were found beside the typical emission peak. These weaker peaks may be closely associated with interstitials of zinc and sulphate ions.

### Thermal Analysis (TGA/DTA)

Thermogravimetric and differential thermal analyses (TGA/DTA) are methods for examining the relationship between the thermophysical and kinetic properties of substances with temperature [37, 38]. The TGA/DTA measurements were carried out in nitrogen gas in the temperature range of 50 °C to 800 °C. The corresponding TGA/DTA curves for the ZTTS samples are displayed in Fig. 7. The TGA trace shows three stages of weight loss from 50 °C to 800 °C. During the first stage, there is a small weight loss between 50–80 °C in the curve this may be due to the release of water molecules from the substance. Another weight loss occurring from 150–185 °C may be due to the partial degradation of the substance. The third stage of weight loss from 230–800 °C may be due to the gradual decomposition of

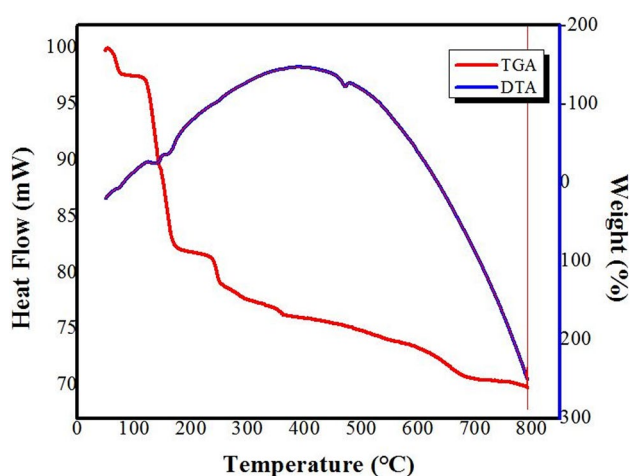


Fig. 7 TGA/DTA curves of ZTTS

the whole substance. The DTA trace illustrates two endothermic peaks during this time, one at 150 °C and the other at 400 °C, which can be explained by partial breakdown followed by total fragmentation of the compound. This leads to the possibility that the ZTTS crystal is thermally stable up to 150 °C.

### SHG Study

Second harmonic generation (SHG) is a nonlinear optical phenomenon whereby photons interact with a nonlinear substance to produce new photons with a frequency that is twice as high as the original photons. The SHG of prepared ZTTS powders was measured by using Kurtz and Perry powder method [39, 40]. The SHG is often carried out by introducing a nonlinear substance into laser light. The generation of an SHG signal depends on the symmetry of the molecules in a sample, and SHG arises if the symmetry is noncentrosymmetric. The ZTTS sample is a suitable substance for SHG since it processes a noncentrosymmetric pattern. For SHG measurements, powdered ZTTS samples were used. In this study, a single-shot mode laser with a fundamental wavelength of 1064 nm, a pulse width of 6 ns, and a repetition rate of 10 Hz was used. The light output of the ZTTS powders was measured using an oscilloscope and photosensitive diode module. The emission of light with a wavelength of 532 nm supports the generation of the second harmonic frequency from the ZTTS samples.

### Conclusions

In the present work, metal-organic single crystals of Zinc (tris)-thiourea sulfate (ZTTS) were produced by the slow evaporation method over 30 days. The ZTTS samples were analyzed by Powder-X-ray crystallography, FT-IR, UV-Vis, PL, TGA/DTA analyses, and SHG determination. Based on XRD analysis, the ZTTS crystallized in an orthorhombic crystal structure. The occurrence of functional groups in the ZTTS was found by FT-IR spectroscopy. According to UV-Vis analysis, the optical transmittance of ZTTS is much higher across the near-UV, visible, and near-IR areas of electromagnetic spectra with the lower cut-off wavelength of 280 nm. This is a useful characteristic of nonlinear optical systems since greater optical transparency in these regions improves the frequency conversion ability. The band gap of ZTTS is determined as 4.43 eV. The photoluminescence characteristics of the as-prepared samples were investigated by PL spectra. A strong emission peak is visible in the PL spectra around 484 nm, and there are significant peaks at 444 and 513 nm with an excitation wavelength of 250 nm. The ZTTS crystal is stable up to

150 °C during TGA-DTA analysis. The results suggest that the produced ZTTS crystals might be advantageous in nonlinear optical applications.

**Author Contribution** Helen Merina Albert: Conceptualization, Data Curation, Supervision, and Validation. T. Jemima: Formal analysis and Investigation, Methodology, Software. C. Alosious Gonsago: Writing-original draft preparation, Visualization, Writing- review and Editing.

**Data Availability Statement** The datasets generated during and/or analyzed during the current study are available from the corresponding author on reasonable request.

## Declarations

**Ethical Approval** This article does not contain any studies with human participants or animals performed by any of the authors.

**Competing Interests** The authors declare that no funds, grants, or other support were received during the preparation of this manuscript.

## References

- Rajkumar M, Chandramohan A (2016) Synthesis, spectral, thermal, mechanical and structural characterization of NLO active organic salt crystal: 3,5-Dimethylpyrazolium-3-Nitrophthalate. *Mater Lett* 181:354–357. <https://doi.org/10.1016/j.matlet.2016.04.191>
- Manivannan M, Jose M (2021) Growth of High-Quality DSTMS Single Crystals with Enhanced Optical Properties for Photonic Applications. *J Electron Mater* 50:1221–1229. <https://doi.org/10.1007/s11664-020-08664-z>
- Sheen Kumar N, Rayar SL (2022) Synthesis, crystal growth and characterization of semi-organic NLO materials: L-valine copper chloride as an optoelectronic sensor. *Ind J Phys* 96:79–87. <https://doi.org/10.1007/s12648-020-01946-6>
- Albert HM, Joseph Arul Pragasam A, Bhagavan Narayana G, Alosious Gonsago C (2014) Investigation on structural, spectral, and thermal properties of L-histidinium glutarate monohydrate (LHG). *J Therm Anal Calorim* 118:333–338. <https://doi.org/10.1007/s10973-014-4007-9>
- Xu K, Cao L, You F, Zhong D, Wang T, Yu Z, Hu C, Tang J, Teng B (2020) Crystal growth and characterization of optical, thermal and electrical properties of organic NLO crystal OHB-T. *J Cryst Grow* 547:125757. <https://doi.org/10.1016/j.jcrysgro.2020.125757>
- Karnan C, Prabakaran A, Prabhakaran M, Vintha G (2019) Growth, Optical, Thermal, Mechanical, Laser Damage Threshold and Electrical Polarizability of Cadmium Chloride Doped L-Alanine (LACC) Single Crystal for Optoelectronic Applications. *J Electron Mater* 48:7915–7922. <https://doi.org/10.1007/s11664-019-07630-8>
- Albert HM, Alosious Gonsago C (2022) Crystallization and Characterization of 2l-Histidinium-2Maleate-3H<sub>2</sub>O and l-Histidinium-Glutarate-H<sub>2</sub>O Organic Crystals for Frequency Conversion Applications. *J Electron Mater* 51:4555–4564. <https://doi.org/10.1007/s11664-022-09712-6>
- Jeyaram J, Varadharajan K, Singaram B, Rajendhran R (2018) Growth and characterization of organic second-order nonlinear optical (NLO) 4-chloroanilinium-l-tartrate monohydrate single crystals. *J Cryst Grow* 486:96–103. <https://doi.org/10.1016/j.jcrysgro.2018.01.015>
- Kamatchi K, Umarani P, Radhakrishnan T, Ramachandra Raja C (2018) Investigation on organic-inorganic hybrid NLO crystal L-Valine Potassium Penta Borate octa hydrate (LVPPB) for NLO applications. *Optik* 172:674–679. <https://doi.org/10.1016/j.ijleo.2018.07.054>
- Chandrasekaran J, Ilayabarathi P, Maadeswaran P, Mohamed Kutty P, Pari S (2012) Growth and characterization of l-histidine cadmium chloride monohydrate a semi-organic nonlinear optical crystals. *Opt Commun* 285:2096–2100. <https://doi.org/10.1016/j.optcom.2011.12.063>
- Pal Rathee S, Singh Ahlawat D, Martin Britto Dhas SA, Maurya KK, Singh B, Bdikin I (2021) Investigation on key properties of solution grown l-Leucine hydrobromide single crystal: A semi-organic NLO material. *Mater Sci Eng B* 264:114927. <https://doi.org/10.1016/j.mseb.2020.114927>
- Subhashini R, Arjunan S, Gunasekaran B (2019) Synthesis of a metal coordinated amino acid-based nonlinear single crystal, Bis(l-threonine)zinc(II) using the solution growth technique and its physicochemical properties. *J Phys Chem Sol* 135:109077. <https://doi.org/10.1016/j.jpccs.2019.109077>
- Rajesh NP, Kannan V, Ashok M, Sivaji K, Santhana Raghavan P, Ramasamy P (2004) A new nonlinear optical semi-organic material: cadmium thiourea acetate. *J Cryst Grow* 262:561–566. <https://doi.org/10.1016/j.jcrysgro.2003.10.064>
- Azhar SM, Rabbani G, Shirsat MD, Hussaini SS, Baig MI, Ghramh HA, Anis M (2018) Luminescence, laser induced nonlinear optical and surface microscopic studies of potassium thiourea chloride crystal. *Optik* 165:259–265. <https://doi.org/10.1016/j.ijleo.2018.03.098>
- Srinivasan BR, Naik TA, Tylczy Z, Ski A, Priolkar KR (2014) Reinvestigation of growth of thiourea urea zinc sulfate crystal. *Spectrochim Acta A* 117:805–809. <https://doi.org/10.1016/j.saa.2013.08.083>
- Suresh S (2014) Studies on the optical and dielectric properties of a zinc thiourea chloride NLO single crystal. *Optik* 125:1223–1226. <https://doi.org/10.1016/j.ijleo.2013.07.154>
- Anis M, Hussaini SS, Hakeem A, Shirsat MD, Muley GG (2016) Synthesis, growth and optical studies of novel organometallic NLO crystal: Calcium bis-thiourea chloride. *Optik* 127:2137–2142. <https://doi.org/10.1016/j.ijleo.2015.11.097>
- Ushasree PM, Muralidharan R, Jayavel R, Ramasamy P (2000) Growth of bis (thiourea) cadmium chloride single crystals-a potential NLO material of organometallic complex. *J Cryst Grow* 218:365–371. [https://doi.org/10.1016/S0022-0248\(00\)00593-5](https://doi.org/10.1016/S0022-0248(00)00593-5)
- Raja Shekar PV, Nagaraju D, Sateesh Chandra Ch, Madhavi Latha D, Kishan Rao K (2020) Investigations on surface and mechanical properties of bis-thiourea cadmium iodide –A nonlinear optical crystal. *Sol State Sci* 107:106353. <https://doi.org/10.1016/j.solidstatesciences.2020.106353>
- Rajagopalan NR, Krishnamoorthy P, Jayamoorthy K, Austeria M (2016) Bis (thiourea) strontium chloride as promising NLO material: An experimental and theoretical study. *Karb Internat J Mod Sci* 2:219–225. <https://doi.org/10.1016/j.kijoms.2016.08.001>
- Pabitha G, Dhanasekaran R (2013) Investigation on the linear and nonlinear optical properties of a metal organic complex-Bis thiourea zinc acetate single crystal. *Opt Las Technol* 50:150–154. <https://doi.org/10.1016/j.optlastec.2013.03.004>
- Ilango E, Rajasekaran R, Krishnan S, Chithambaram V (2014) Growth and characterization of bis(thiourea) zinc carbonate (BTZC) a new nonlinear optical material by solution growth slow evaporation technique. *Optik* 125:7113–7115. <https://doi.org/10.1016/j.ijleo.2014.08.113>
- Srineevasan R, Rajasekaran R (2013) Growth and optical studies of 2-aminopyridine bis thiourea zinc sulphate (2-APTZS) single crystals for NLO applications. *J Mole Struct* 1048:238–243. <https://doi.org/10.1016/j.molstruc.2013.05.052>

24. Bhuvanewari N, Baskar K, Dhanasekaran R (2015) Growth and characterization of tris thiourea magnesium zinc sulphate single crystals. *Optik* 126:3731–3736. <https://doi.org/10.1016/j.ijleo.2015.08.246>
25. Revathi V, Karthik K, Mahdizadeh H (2019) Antibacterial activity and physico-chemical properties of metal-organic single crystal: Zinc (Tris) thiourea chloride. *Chem Data Coll* 24:100279. <https://doi.org/10.1016/j.cdc.2019.100279>
26. Jalel B, Ennaceur N, Hawech S, Henchiri R, Bouguerra W, Ledoux-Rak I (2019) Synthesis and characterization of a metal-organic NLO material: Tetrakis (thiourea) cobalt chloride. *J Phys Chem Soli* 133:35–44. <https://doi.org/10.1016/j.jpcs.2019.04.036>
27. Andreotti GD, Cavalca L, Musatti A (1968) The crystal and molecular structure of tris (thiourea) zinc(II) sulphate. *Acta Cryst B* 24:683–690. <https://doi.org/10.1107/S056774086800302X>
28. Alosious Gonsago C, Albert HM, Kathikeyan J, Sagayaraj P, Joseph Arul Pragasam A (2012) Crystal structure, optical and thermal studies of a new organic nonlinear optical material: L-Histidinium maleate 1.5-hydrate. *Mater Res Bull* 47:1648–1652. <https://doi.org/10.1016/j.materresbull.2012.03.061>
29. Albert HM, Lohitha T, Alagesan K, Alosious Gonsago C, Vinita V (2021) Performance of ZnSO<sub>4</sub> doped CeO<sub>2</sub> nanoparticles and their antibacterial mechanism. *Mater Tod Proceed* 47:1030–1034. <https://doi.org/10.1016/j.matpr.2021.06.124>
30. Ushasree PM, Jayavel R, Subramanian C, Ramasamy P (1999) Growth of zinc thiourea sulfate (ZTS) single crystals- a potential semiorganic NLO material. *J Cryst Grow* 197:216–220. [https://doi.org/10.1016/S0022-0248\(98\)00906-3](https://doi.org/10.1016/S0022-0248(98)00906-3)
31. Herzberg G, Crawford BL Jr (1946) Infrared and Raman Spectra of Polyatomic Molecules. *J Phys Chem* 50:288. <https://doi.org/10.1021/j150447a021>
32. Özbek FE, Sertçelik M, Yüksek M, Uğurlu G, Tonbul AM, Necefoglu H, Hökelek T (2019) Synthesis and Crystallographic, Absorption and Emission Studies of 4-Pyridine Carboxamide of Zn(II) 4-Chlorophenylacetate. *J Fluoresc* 29:1265–1275. <https://doi.org/10.1007/s10895-019-02440-x>
33. Atuchin VV, Subanakov AK, Aleksandrovsky AS, Bazarov BG, Bazarova JG, Dorzhieva SG, Gavrilova TA, Krylov AS, Molokeyev MS, Oreshonkov AS, Pugachev AM, Tushinova YL, Yelissev AP (2017) *Adv Powd Technol* 28:1309–1315. <https://doi.org/10.1016/j.apt.2017.02.019>
34. Bassey VM, Apebende CG, Idante PS et al (2022) Vibrational Characterization and Molecular Electronic Investigations of 2-acetyl-5-methylfuran using FT-IR, FT-Raman, UV-VIS, NMR, and DFT Methods. *J Fluoresc* 32:1005–1017. <https://doi.org/10.1007/s10895-022-02903-8>
35. Archana R, Sudhahar S, Sadayandi K, Vidhya M, Sagadevan S, Mohammad F, Podder J (2020) Investigation of the optical, photoluminescence, and dielectric properties of *P*-Toluidinium picrate single crystals. *Chine J Phys* 67:283–292. <https://doi.org/10.1016/j.cjph.2020.07.010>
36. Christina Rhoda J, Chellammal S, Albert HM, Ravichandran K, Alosious Gonsago C (2023) Synthesis, Spectroscopic, and Antibacterial Characterizations of Cadmium-Based Nanoparticles. *J of Fluoresc*. <https://doi.org/10.1007/s10895-023-03290-4>
37. Gora MK, Kumar A, Kumar S, Nehra J, Lal Choudhary B, Dolia SN, Singhal RK (2023) The study of optical, structural and magnetic properties of Cu-doped ZnO nanoparticles. *J Mater Sci: Mater Electron* 34:288. <https://doi.org/10.1007/s10854-022-09713-5>
38. Castro RI, Gallego J, García MF, Marican A, Doria OF (2021) Thermal study and composition of edible oils combined by TG/DTG analysis through predictive statistical model. *J Therm Anal Calorim* 145:153–160. <https://doi.org/10.1007/s10973-020-09693-w>
39. Kurtz SK, Perry TT (1968) A Powder Technique for the Evaluation of Nonlinear Optical Materials. *J Appl Phys* 39:3798–3813. <https://doi.org/10.1063/1.1656857>
40. Albert HM, Alosious Gonsago C (2022) Comparative studies on formation and material characterization of L-histidine derivatives for nonlinear optical device applications. *J Mater Sci Mater Electron* 33:2970–2979. <https://doi.org/10.1007/s10854-021-07495-w>

**Publisher's Note** Springer Nature remains neutral with regard to jurisdictional claims in published maps and institutional affiliations.

Springer Nature or its licensor (e.g. a society or other partner) holds exclusive rights to this article under a publishing agreement with the author(s) or other rightsholder(s); author self-archiving of the accepted manuscript version of this article is solely governed by the terms of such publishing agreement and applicable law.